WORM COIL DISTRIBUTION AND LOAD-CARRYING ABILITY FOR AN ELECTROMECHANICAL INTEGRATED TOROIDAL DRIVE

Lizhong Xu and Dazhou Zheng
Mechanical engineering institute, Yanshan University, Qinhuangdao, Hebei, 066004, China

Received November 2005, Accepted March 2009
No. 05-CSME-60, E.I.C. Accession 2912

ABSTRACT

This paper investigates worm coil distribution and load-carrying ability for a toroidal drive. The lead angle equations for the worm groove are given for different coil distributions. The center curve of the worm groove is obtained using coordinate transformation. A 3D worm model is constructed using Pro/Engineer software and the average output torque is presented to compare load-carrying ability for the drive with different worm coil distributions. As the number of the planet teeth increases, the output torque of the drive first increases then decreases. Large output torque requires an optimum number of planet teeth and a larger number of pole pairs and stator teeth.

Keywords: toroidal drive, electromechanical integrated, coil distribution, output torque.

DISTRIBUTION PAR VIS SANS FIN ET CAPACITÉ DE CHARGE D'UN VARIATEUR TOROÏDAL ÉLECTRO-MÉCANIQUE INTÉGRÉ

RÉSUMÉ

L'article étudie la distribution par vis sans fin et la capacité de charge d'un variateur toroïdal. Les équations de l'angle d'avance pour les cannelures de la vis sont données pour différentes distributions. La courbure du centre de la cannelure est obtenue par changement coordonnée. Un modèle 3D est construit à l'aide du logiciel Pro/Engineer, et la moyenne du couple de sortie est présentée pour comparer la capacité de charge du variateur avec différentes distributions par vis sans fin. Comme le nombre de dents planétaires augmente, le couple de sortie du variateur commence par s'accroître puis décroît. Un couple de sortie plus grand requiert un nombre optimal de dents planétaires et un nombre élevé de paires de pôles et de dents au stator.

Mots-clés: variateur toroïdal, électromécanique intégré, distribution par vis sans fin, couple de sortie.

1. INTRODUCTION

Small sized toroidal drives can achieve a large torque are suitable for applications such as aviation and space flight [1–5]. Generalized composite drives technology has advanced recently as more and more electrical and control techniques are used in mechanical engineering design. Recent research on toroidal drives in [6–7] presents an electromechanical integrated toroidal drive, which is a new concept of an active generalized composite drive. In this drive, the toroidal drive, power and control are integrated. Compared with normal toroidal drives, the new drive is easy to produce, does not wear, and does not need lubrication. It can be substituted for a servo system to simplify the structure of existing electromechanical systems. Besides applications that require compactness, the drive can be used in fields such as robots, which require accurate control [8].

The worm coil distributions are classified into two types: (1) planet teeth to partial worm teeth, and (2) worm teeth to partial planet teeth. In this paper, the worm coil distributions and load-carrying ability for the drive are investigated. The research is useful for designing and manufacturing the drive and can be used to calculate the load carrying ability.

2. BASIC PRINCIPLE

The drive consists of four basic elements as shown in Fig. 1(a) – (1) planets; (2) the central worm; (3) a toroidal shaped stator; and (4) a rotor. These elements form the central output shaft upon which the planets are mounted. The central worm is fixed and coils are mounted in helical grooves of its surface. The planets have permanent magnets instead of teeth and the poles of the permanent magnets are mounted alternately on a planet. The stator also has helical permanent magnets instead of helical teeth and the poles of the stator permanent magnets are mounted alternately on the stator.

If a specific parameter relation of the drive system is realized, the N-pole of one element will correspond to S-pole of the other one. The attractive forces between N and S-poles of the different elements are driving forces and meshes without contact are realized. When AC current is applied to the coils of the worm, a toroidal circular field is formed. This field drives several planets to rotate about their own axis. By means of magnetic forces between the teeth of the planet and stator, the rotor is driven to rotate about its own axes. Thus, the drive produces a large torque at a low speed.

If the gear reduction ratio i_{wr} of the drive is defined as the ratio of the rotational magnetic field speed to the rotor speed, then it can be expressed as:

$$i_{wr} = \frac{\omega_w}{\omega_r} = 1 \pm \frac{z_0}{2p} \tag{1}$$

where ω_w is rotational speed of the electromagnetic field, ω_r is the speed of the rotor, z_0 is the number of stator teeth, and p is the number of the pole pairs of the worm coils.

In Eq. (1), a positive sign corresponds to when the lead angles are in the same direction for the worm and stator, and a negative sign to when the lead angles are opposing.

From the relations between the relative motion of the stator, worm and planet, and the condition that along the length of the drive the N-pole of one element should correspond to S-pole of another element, mounting condition of the drive is obtained as:

$$m = \frac{2p + z_0}{N} \tag{2}$$

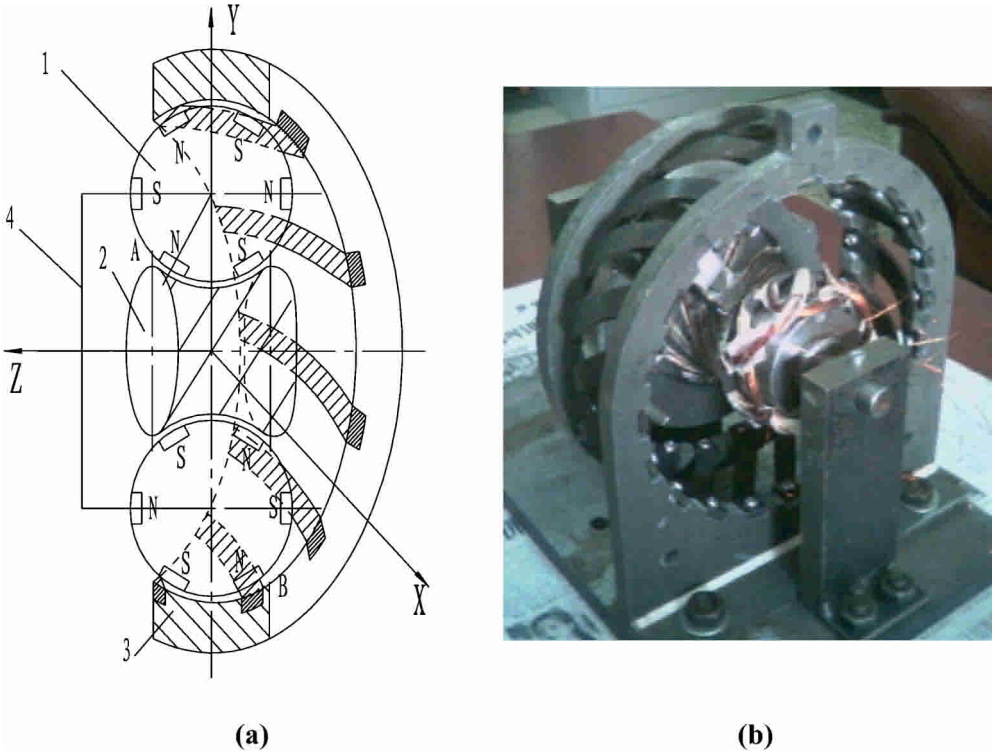

Fig. 1. Electromechanical integrated toroidal drive: (a) drive diagram (b) model machine of the drive.

where m is the planet number and N is a positive integer.

If $p = 1$, the stator is divided into two parts by the pole pair. If the number of the stator teeth is increased, the number of the N and S-pole pairs should be increased in each part. Therefore the increase in the number of stator teeth should be a multiple of four and is equal to $4n$ (where $n = 0, 1\ldots$) and the number of the stator teeth is given by:

$$z_0 = 2 + 4n = 2(1 + 2n) \tag{3}$$

If $p = 2$, the stator is divided into four parts. If the number of the stator teeth is increased, the number of N and S-pole pairs should be increased in each part as well. Therefore the increase in the number of stator teeth should be multiple of eight and is equal to $8n$ (where $n = 0, 1\ldots$) and the number of the stator teeth is given by:

$$z_0 = 4 + 8n = 4(1 + 2n) \tag{4}$$

Hence, the number of the stator teeth should be taken as:

$$z_0 = 2p(1 + 2n) \tag{5}$$

where n is positive integer.

According to the condition that circular pitches of the stator, worm, and planet should be equal in the normal line direction of the teeth surface, the correct meshing condition of the drive is obtained as:

$$z_0/tg\lambda_s = 2p/tg\lambda_w + 2z_1 \tag{6}$$

where z_1 is the number of the planet teeth, λ_s is the lead angle of the stator tooth, and λ_w is the lead angle of the worm groove.

3. WORM COIL DISTRIBUTIONS AND LEAD ANGLES

The central worm consists of a number of silicon steel sheets. Several helical slots are cut on the worm and insulated wire windings are mounted into these helical slots. From Fig. 2, it can be seen that rotating the coils from one end of the worm to another causes the single pole pair magnetic field to become a multi-pole pair magnetic field. In Fig. 2, the figure on the left shows a single pole pair magnetic field before a coil rotation and it shows the side surface magnetic field after a coil rotation. The figure on the right shows a multi-pole pair magnetic field after the coil rotation.

The coil distribution on the worm can be represented by the lead angle. The lead angle is decided by the number of the pole pairs of the coils, the number of planet teeth and other parameters. The coil distribution is clasified into two types: (1) planet teeth to partial worm teeth, and (2) worm teeth to partial planet teeth.

3.1 Planet teeth to partial worm teeth

Fig. 3 shows the coil distribution under the condition that $z_1 = 6$ and $p = 1$. In Fig. 3(a), one pair of the planet teeth corresponds to one pair of the worm teeth. In Fig. 3(b), one pair of the planet teeth corresponds to two pairs of the worm teeth among which one pair of the teeth is idle.

Fig. 3 shows that when the planet rotates one tooth space (60°), the corresponding worm tooth rotates one polar distance (180°), under the condition that there is no idle worm tooth between two adjacent planet teeth. Under the condition that there is one pair of idle worm teeth between two adjacent planet teeth, when the planet rotates one tooth space (60°), the corresponding worm tooth rotates (2+1) polar distances (540°).

If ϕ_0 denotes the central angle of two adjacent teeth for a planet, then:

$$\varphi_0 = 360^\circ/z_1 \tag{7}$$

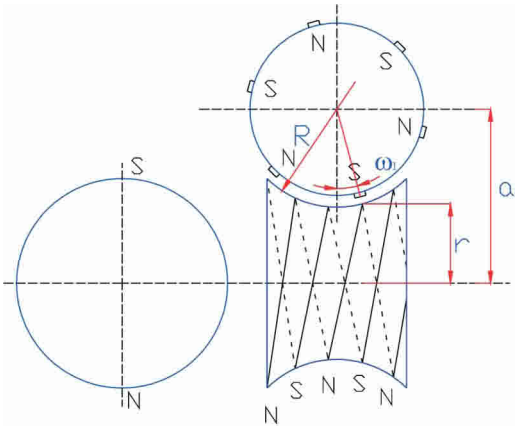

Fig. 2. Multi-pole pair magnetic field after a coil rotation.

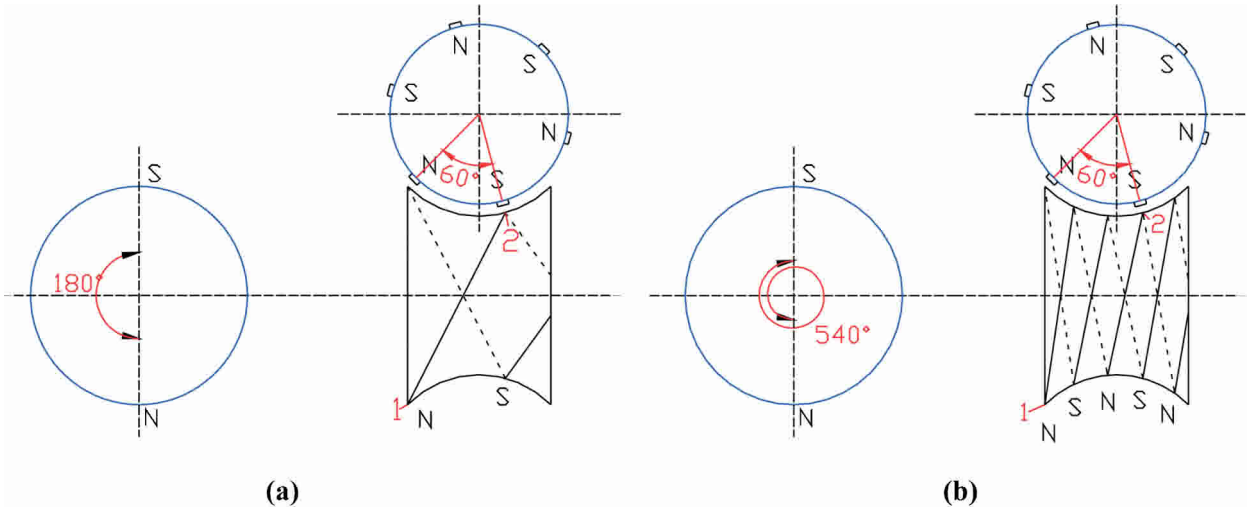

Fig. 3. Coil distributions on the worm with $p = 1$ and $z_1 = 6$.

and if ϕ_{w0} denote central angle of two adjacent poles for the worm, then:

$$\varphi_{w0} = \frac{360^\circ}{2p} = \frac{180^\circ}{p} \tag{8}$$

Thus, under the condition that there are n pairs of idle worm teeth between two adjacent planet teeth, then when planet rotates one tooth space (ϕ_0), the corresponding worm tooth rotates ($2n + 1$) polar distances (($2n + 1)\phi_{w0}$). Therefore this type of coil distribution is denoted as *planet teeth to partial worm teeth*. For this situation, the lead angle λ_w of the worm groove can be calculated as:

$$\tan\lambda_w = \frac{\varphi_0 R}{(2n+1)\varphi_{w0} r} = \frac{2pR}{z_1(2n+1)r} = \frac{2p}{z_1(2n+1)(a/R - \cos\varphi_1)} \tag{9}$$

where R is the planet radius, a is the center distance between the planet and worm, r is the radius at some one point of the worm, $r = a - R\cos\phi_1$, and ϕ_1 is the rotating angle of the planet, as shown in Fig. 2.

Using Eq.(9), the coil distribution of the worm with $p = 2$ can be given as shown in Fig. 4.

In Fig. 4(a), when the planet rotates one tooth space (60°), the corresponding worm tooth rotates one polar distance ($\phi_{w0} = 90^\circ$). In Fig. 4(b), under the condition that there is one pair of idle worm teeth between two adjacent planet teeth, then when the planet rotates one tooth space (60°), the corresponding worm tooth rotates (2+1) polar distances (270°).

3.2 Worm teeth to partial planet teeth

Fig. 5 shows the coil distribution under the condition that the worm coil pole pair number $p = 1$ and its helical tooth distance equals 60°. In Fig. 5(a), one pair of the worm teeth corresponds to one pair of the planet teeth. In Fig. 5(b), one pair of the worm teeth corresponds to two pairs of the planet teeth among which one pair of the teeth is idle.

Fig. 5(a) shows that when the worm tooth rotates one polar distance (180°), the planet rotates one tooth space (60°). Fig. 5(b) shows that under the condition that there is one pair of

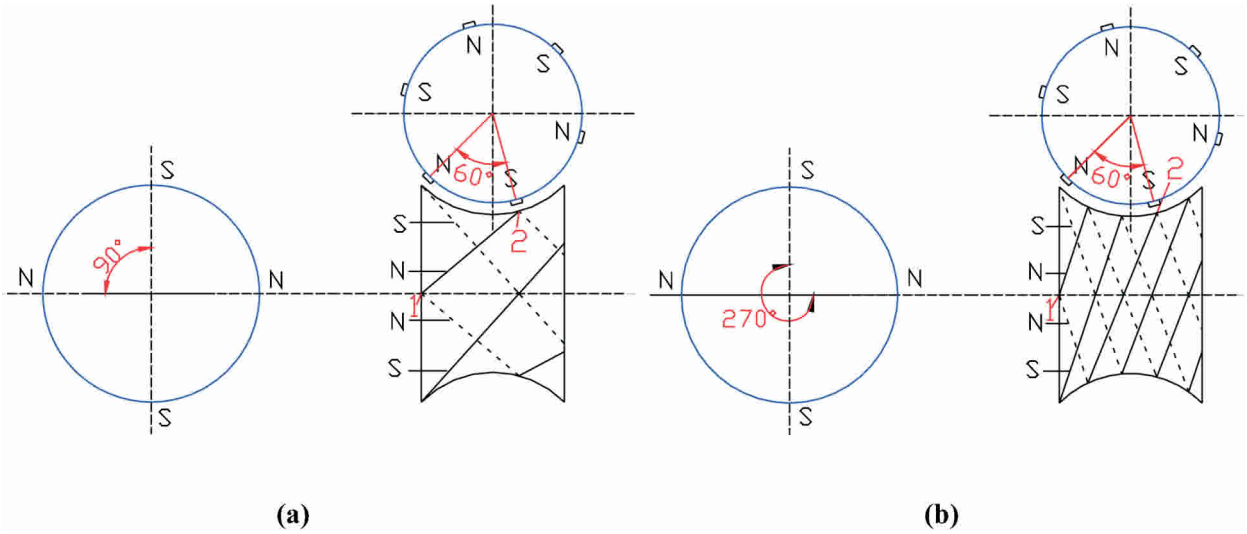

Fig. 4. Coil distribution on the worm under $p = 2$ and $z_1 = 6$.

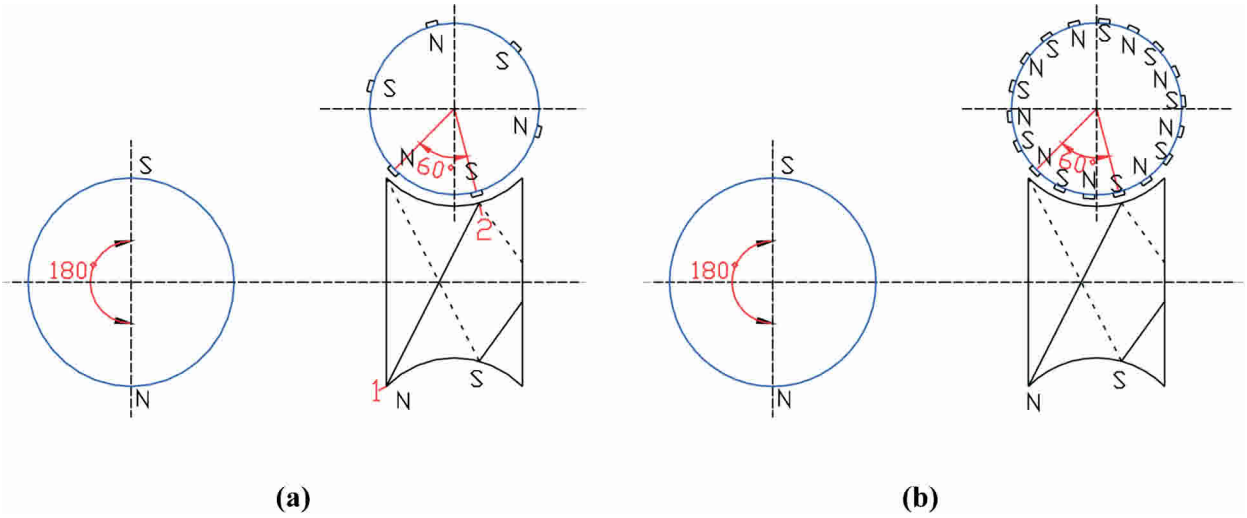

Fig. 5. Coil distribution on the worm with $p = 1$ and a 60° helical tooth distance.

idle planet teeth between two adjacent worm teeth, then when the worm tooth rotates one polar distance (180°), the planet still rotates 60° but it corresponds to (2+1) planet tooth spaces (where the planet tooth space angle $\phi_0 = 20°$).

Thus, under the condition that there are n pairs of idle planet teeth between two adjacent worm teeth, when the worm rotates one polar space (ϕ_{w0}), the corresponding planet tooth rotates $(2n + 1)$ tooth spaces ($(2n + 1)\phi_0$). This type of coil distribution is denoted as *worm teeth to partial planet teeth*. For this situation, the lead angle λ_w of the worm groove can be calculated as:

$$\tan \lambda_w = \frac{(2n+1)\varphi_0 R}{\varphi_{w0} r} = \frac{2p(2n+1)R}{z_1 r} = \frac{2(2n+1)p}{z_1(a/R - \cos \varphi_1)} \tag{10}$$

Using Eq.(10), the coil distribution of the worm with $p = 2$ can be given as shown in Fig. 6.

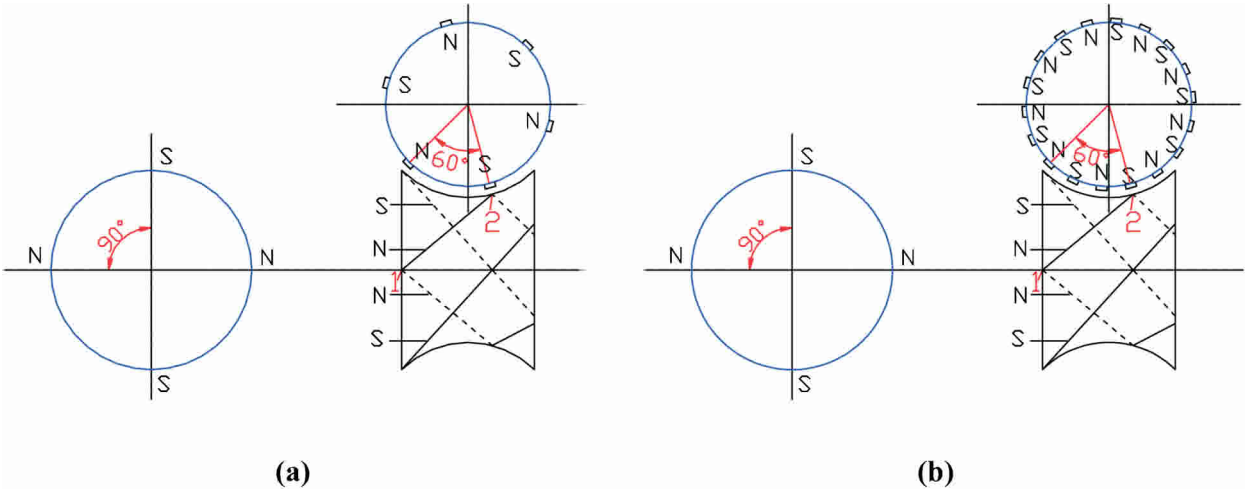

Fig. 6. Coil distribution on the worm under $p = 2$ and a 60° helical worm tooth distance.

In Fig. 6(a), when the worm rotates one polar space (90°), the corresponding planet tooth rotates one tooth space ($\phi_0 = 60°$). In Fig. 6(b), under the condition that there is one pair of idle planet teeth between two adjacent worm teeth, when the worm rotates one polar space (90°), the corresponding planet tooth rotates (2+1) tooth spaces (60°).

3.3 Planet teeth to worm teeth

In Eqs. (9) and (10), if $n = 0$ then Eq.(9) is identical with Eq.(10) and Eqs. (9) and (10) are transformed into:

$$\tan \lambda_w = \frac{2p}{z_1(a/R - \cos \varphi_1)} \tag{11}$$

This type of worm coil distribution is denoted as *planet teeth to worm teeth*. For this coil distribution, each planet tooth corresponds to one worm tooth and there are no idle teeth in the planet or worm.

Substituting Eq.(11) into (6), the lead angle λ_s of the helical tooth for the stator can be given as:

$$\tan \lambda_s = \frac{2p(2N+1)}{z_1(a/R - \cos \varphi_1 + 2)} \tag{12}$$

4. SOLID MODEL OF THE WORM

The coordinate systems for the drive are represented in Fig. 7. The coordinate system $s(x, y, z)$ is attached to the stator, $s_1(x_1, y_1, z_1)$ to the planet, $s_2(x_2, y_2, z_2)$ to the worm, and $s_r(x_r, y_r, z_r)$ to the rotor. The reference coordinate system $s_{10}(x_{10}, y_{10}, z_{10})$ is attached to the rotor. The z_2-axis and z_r-axis are the rotating axes of the worm and the rotor, respectively. The z_1-axis is the rotating axis of the planet and ϕ_1, ϕ_2 and ϕ_r are the rotating angles of the planet, worm, and rotor, respectively.

From Fig. 7, it is known that in coordinate system s_1, the center of the planet tooth can be calculated as:

$$\begin{cases} x_1 = R \\ y_1 = 0 \\ z_1 = 0 \end{cases} \tag{13}$$

The center of the planet tooth is transformed to system $s_2(x_2, y_2, z_2)$ and the center of the worm groove can be obtained as:

$$\begin{bmatrix} x_2 \\ y_2 \\ z_2 \end{bmatrix} = \mathbf{M}_{20}\mathbf{M}_{0r}\mathbf{M}_{r10}\mathbf{M}_{101} \begin{bmatrix} x_1 \\ y_1 \\ z_1 \end{bmatrix} \tag{14}$$

Where $\mathbf{M}_{101}$ is the coordinate transformation matrix from coordinate system s_1 to system s_{10}. $\mathbf{M}_{r10}$, $\mathbf{M}_{0r}$ and $\mathbf{M}_{20}$ are coordinate transformation matrices from the coordinate system s_{10} to system s_r, from s_r to s, and from s to s_1, respectively, and are given as:

$$\mathbf{M}_{101} = \begin{bmatrix} \cos\varphi_1 & -\sin\varphi_1 & 0 \\ \sin\varphi_1 & \cos\varphi_1 & 0 \\ 0 & 0 & 1 \end{bmatrix}, \quad \mathbf{M}_{r10} = \begin{bmatrix} 1 & 0 & 0 & a \\ 0 & 0 & 1 & 0 \\ 0 & 1 & 0 & 0 \\ 0 & 0 & 0 & 1 \end{bmatrix}, \quad \mathbf{M}_{0r} = \begin{bmatrix} \cos\varphi_r & -\sin\varphi_r & 0 \\ \sin\varphi_r & \cos\varphi_r & 0 \\ 0 & 0 & 1 \end{bmatrix},$$

$$\mathbf{M}_{20} = \begin{bmatrix} \cos\varphi_2 & -\sin\varphi_2 & 0 \\ \sin\varphi_2 & \cos\varphi_2 & 0 \\ 0 & 0 & 1 \end{bmatrix}$$

Substituting $\mathbf{M}_{101}$, $\mathbf{M}_{r10}$, $\mathbf{M}_{0r}$ and $\mathbf{M}_{20}$ into (14), the center curve of the worm groove can be given as:

$$\begin{cases} x_2 = (R\cos\varphi_1 + a)\cos(\varphi_r - \varphi_2) \\ y_2 = (R\cos\varphi_1 + a)\sin(\varphi_r - \varphi_2) \\ z_2 = R\sin\varphi_1 \end{cases} \tag{15}$$

where $\phi_2 = (1 + z/2p)\phi_r$, the span of the angle ϕ_1 is $[-\phi_{v2}/2, \phi_{v2}/2]$, and ϕ_{v2} is the center angle on the part of the planet enveloped by the worm. The angle ϕ_{v2} and the coordinate system $s_2(x_2, y_2, z_2)$ of the worm are shown in Fig. 8.

The helical centre line of the worm groove is generated, using Eq.(15), as the planet angle ϕ_1 progresses from $-\phi_{v2}/2$ to $\phi_{v2}/2$. A curved worm groove is created as follows: using this centre curve, a single entire worm groove is constructed by extruding along it an appropriate rectangle to represent the groove cross section. Then the groove is duplicated the required number of times in a suitable, uniformly spaced circular pattern. Using Pro/Engineer software, (1) A single worm groove is the result of a "Pro/Engineer helical sweep" command and (2) the complete worm is modeled with a "Pro/Engineer pattern" command.

5. THE OUTPUT TORQUE

From reference [8], the output torque T_n for the drive is given as below:

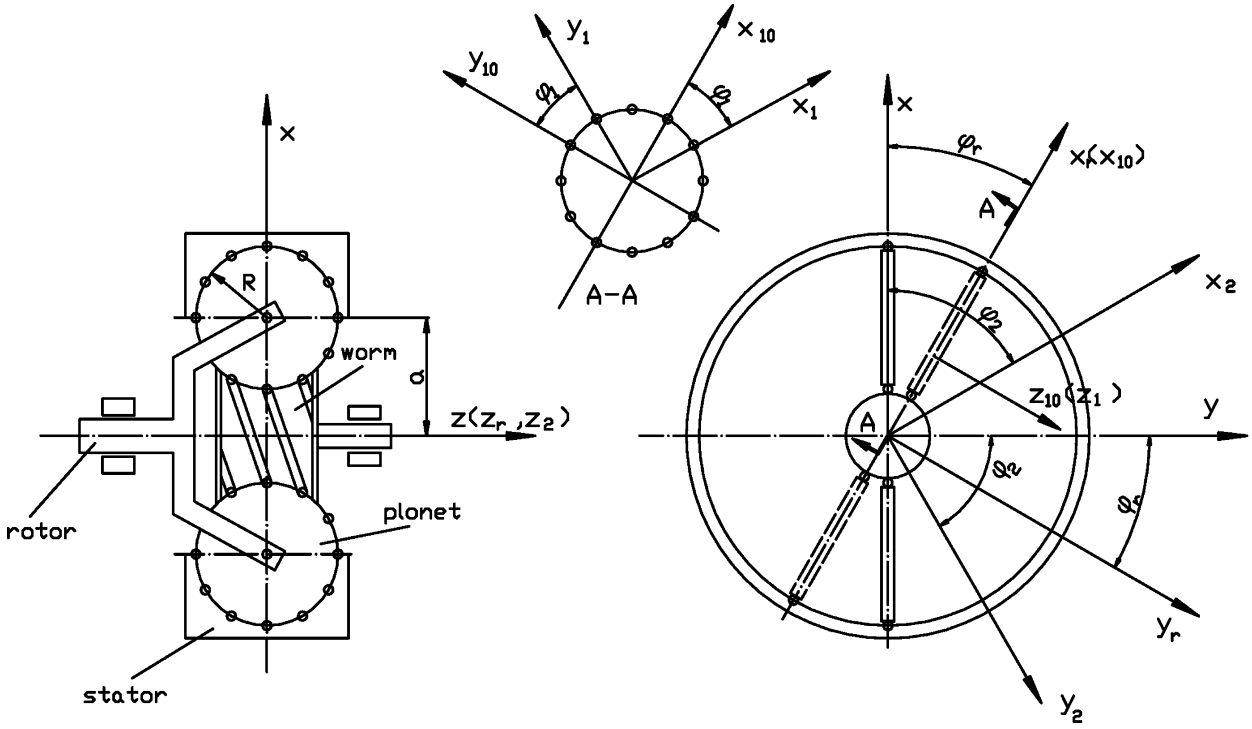

Fig. 7. Coordinate systems for the drive.

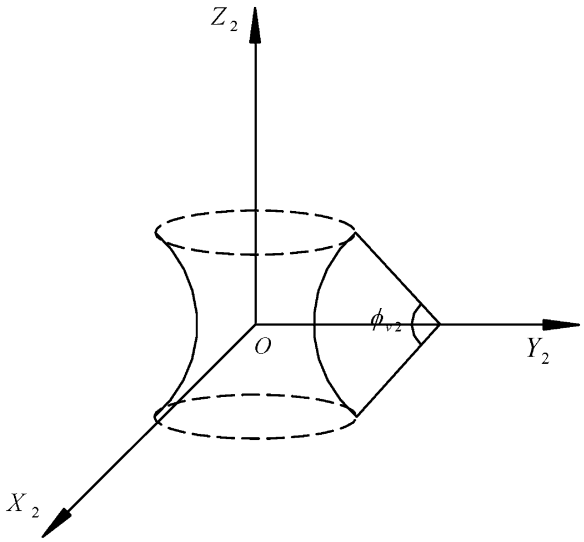

Fig. 8. Coordinate system for the worm.

$$T_n = \frac{1}{2} k_v m q R F_g^2 \frac{d\Lambda_g}{d\zeta} \left(\frac{2p + z_0}{z_1} \right) \sum_{i=1}^{z_v} \frac{1}{\sqrt{1 + \frac{z_1^2}{4p^2} \left(\frac{a}{R} - \cos \varphi_1 \right)^2}} \tag{16}$$

where k_v is distributed winding coefficient, q is the number of turns per worm pole, F_g is the magnetic potential, $F_g = nI$ where n is the turn number of the coil and I is the current intensity,

Λ_g is the air gap magnetic conductance, ζ is the relative displacement between two sides of the air gap, and z_v is number of teeth on the part of the planet enveloped by the worm.

From this analysis, it is known that the number of meshing teeth varies as the drive operates. The fluctuation of the number of teeth in the mesh causes fluctuation of the output torque. In order to compare the load-carrying ability of the drive, the average torque should be given. The average torque T_a can be calculated as:

$$T_a = \frac{1}{2\pi}\int_0^{2\pi} T_n d\varphi_1 \tag{17}$$

6. RESULTS AND DISCUSSION

6.1 Worm coil distribution

Using Eqs.(11) and (12), the lead angles of the worm coils and stator teeth can be calculated under the assumption that there are no idle tooth pairs. Tables 1 and 2 show the lead angles of the worm coils and stator teeth with $p = 1$ and $p = 2$ (where the planet rotating angle $\phi_1 = 0^\circ$). Fig. 9 shows coil distributions corresponding to Table 1.

Table 1 The lead angle of the worm coils and stator teeth ($p = 1$).

Z_1	6	8	10	12	14	16	18
$\tan\lambda_2$	$\frac{1}{3(\frac{a}{R}-1)}$	$\frac{1}{4(\frac{a}{R}-1)}$	$\frac{1}{5(\frac{a}{R}-1)}$	$\frac{1}{6(\frac{a}{R}-1)}$	$\frac{1}{7(\frac{a}{R}-1)}$	$\frac{1}{8(\frac{a}{R}-1)}$	$\frac{1}{9(\frac{a}{R}-1)}$
$\tan\lambda_0$	$\frac{(2N+1)}{3+3(\frac{a}{R})}$	$\frac{(2N+1)}{4+4(\frac{a}{R})}$	$\frac{(2N+1)}{5+5(\frac{a}{R})}$	$\frac{(2N+1)}{6+6(\frac{a}{R})}$	$\frac{(2N+1)}{7+7(\frac{a}{R})}$	$\frac{(2N+1)}{8+8(\frac{a}{R})}$	$\frac{(2N+1)}{9+9(\frac{a}{R})}$

Table 2 The lead angles of the worm coils and stator teeth ($p = 2$).

Z_1	6	8	10	12	14	16	18
$\tan\lambda_2$	$\frac{2}{3(\frac{a}{R}-1)}$	$\frac{1}{2(\frac{a}{R}-1)}$	$\frac{2}{5(\frac{a}{R}-1)}$	$\frac{1}{3(\frac{a}{R}-1)}$	$\frac{2}{7(\frac{a}{R}-1)}$	$\frac{2}{8(\frac{a}{R}-1)}$	$\frac{2}{9(\frac{a}{R}-1)}$
$\tan\lambda_0$	$\frac{2(2N+1)}{3+3(\frac{a}{R})}$	$\frac{2(2N+1)}{4+4(\frac{a}{R})}$	$\frac{2(2N+1)}{5+5(\frac{a}{R})}$	$\frac{2(2N+1)}{6+6(\frac{a}{R})}$	$\frac{2(2N+1)}{7+7(\frac{a}{R})}$	$\frac{2(2N+1)}{8+8(\frac{a}{R})}$	$\frac{2(2N+1)}{9+9(\frac{a}{R})}$

Tables 1, 2 and Fig. 9 show:

(1) As planet tooth number increases, the lead angles of the worm coils and stator teeth decrease and the mesh tooth pair number between the planet and worm increases.
(2) As the ratio a/R increases, the lead angles of the worm coils and stator teeth decrease and the mesh tooth pair number between the planet and worm increases.

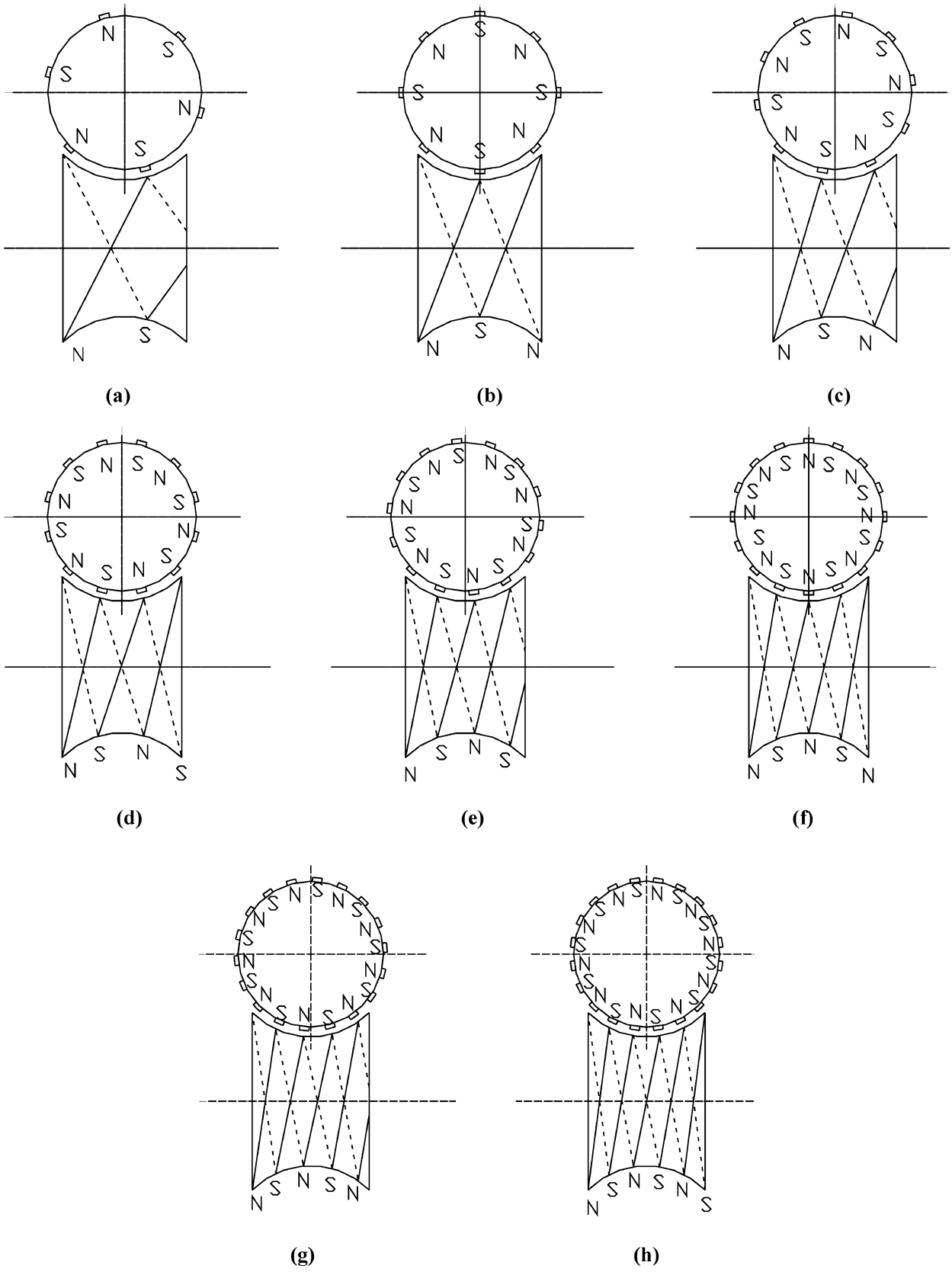

Fig. 9. The coil distribution with no idle tooth pair($n = 0$, $p = 1$). (a) $z_1 = 6$, (b) $z_1 = 6$, (c) $z_1 = 10$, (d) $z_1 = 12$, (e) $z_1 = 14$, (f) $z_1 = 16$, (g) $z_1 = 18$, (h) $z_1 = 20$.

(3) As the pole pair number increases, the lead angles of the worm coils and stator teeth increase. A greater number of pole pairs will produce a greater number of meshing tooth pairs.
(4) Assuming no idle tooth pairs, when the positive integer N is increased, the number of stator teeth is increased and the gear reduction ratio is increased to produce greater torque at a lower output speed, without a change in the number of worm coils.

6.2 The number and size of the worm groove

Using the method given in section 4, several 3D worm models are shown in Fig. 10. In Fig. 10(a), (b) and (c), there is no idle tooth pair ($n = 0$**).** In Fig. 10(d), there is one idle tooth pair ($n = 1$).

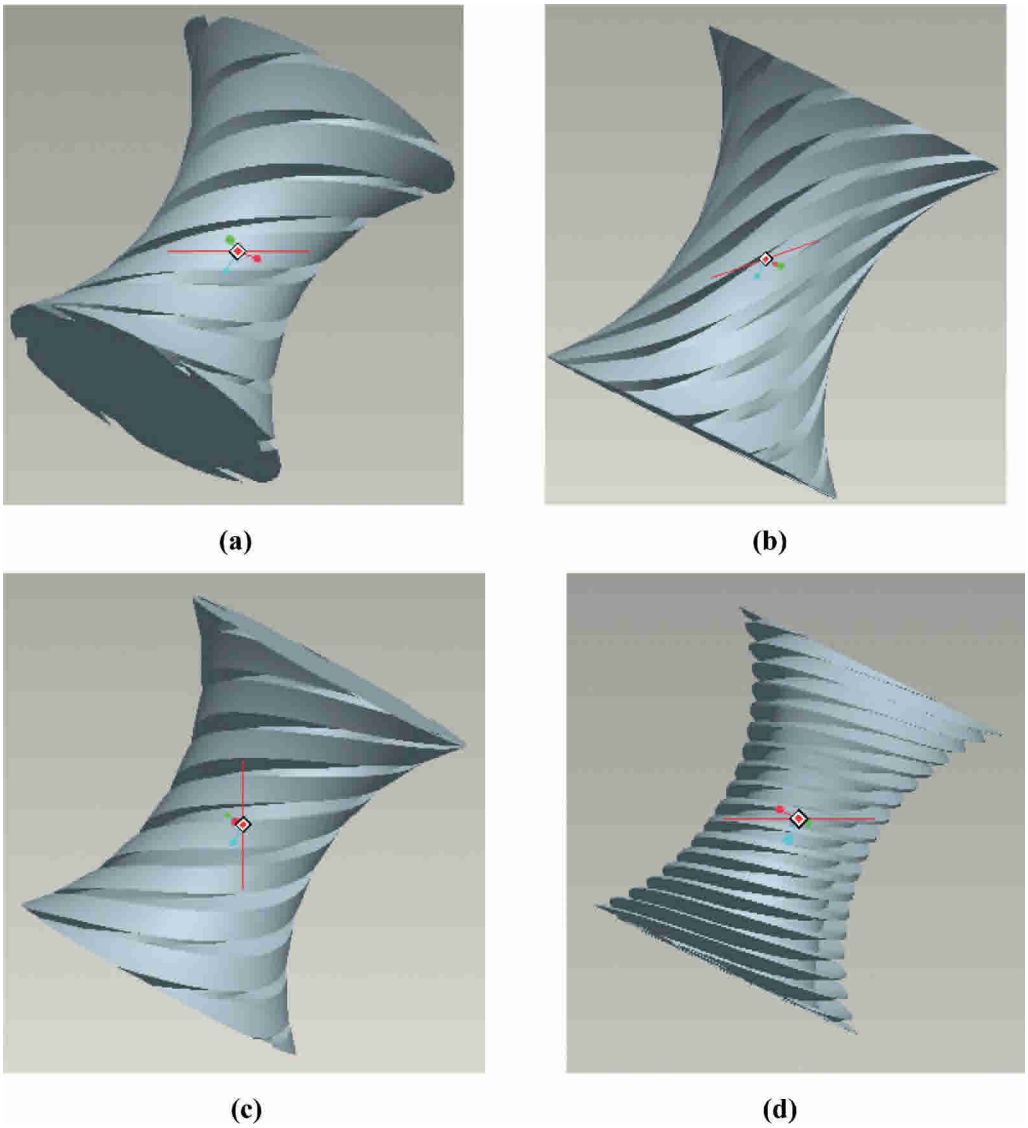

Fig. 10. Solid models of the worm. (a) $p = 1$ $Z_1 = 8$, (b) $p = 2$ $Z_1 = 8$, (c) $p = 1$ $Z_1 = 10$, (d) $p = 1$ $Z_1 = 8$, $n = 1$.

Fig. 10 shows:

(1) As the pole pair number increases, the number of the worm groove increases and the groove cross section size decreases correspondingly.

(2) As the planet tooth number increases, the number of the worm groove increases and the groove cross section size decreases proportionally.

(3) As the idle worm tooth pair increases, the number of the worm groove increases and the groove cross section size decreases correspondingly.

6.3 Output torque

The output torques of the toroidal drive with different worm coils are determined using Eqs.(16) and (17). The relation of the output torque with the planet tooth number and pole pair number is shown in Fig. 11(a). When $p = 1$, the relation of the output torque along with the planet tooth number and stator tooth number is shown in Fig. 11(b).

Fig. 11 shows:

(1) As the planet tooth number increases, the output torque of the drive first increases proportionally, reaches a maximum value, and then decreases rapidly. This is because the groove size of the worm coils decreases and the mesh tooth pair number increases with increasing planet tooth number. The increase of the mesh tooth pair number favors an increase in the output torque. However, decreasing the worm coil groove size will cause a decrease in the output torque. Therefore under a given condition, there is an optimum planet tooth number corresponding to the maximum output torque.

(2) As the pole pair number increases, the output torque of the drive increases. This is because the lead angle of the worm coils increases with increasing pole pair number of the worm coils. A greater lead angle favors an increase in the output torque for the drive system.

(3) For larger pole pair number, the optimum planet tooth number becomes smaller. This is because the worm coil groove number increases with an increase in the pole pair number, the increase of the coil groove number causes a decrease in the size of the groove.

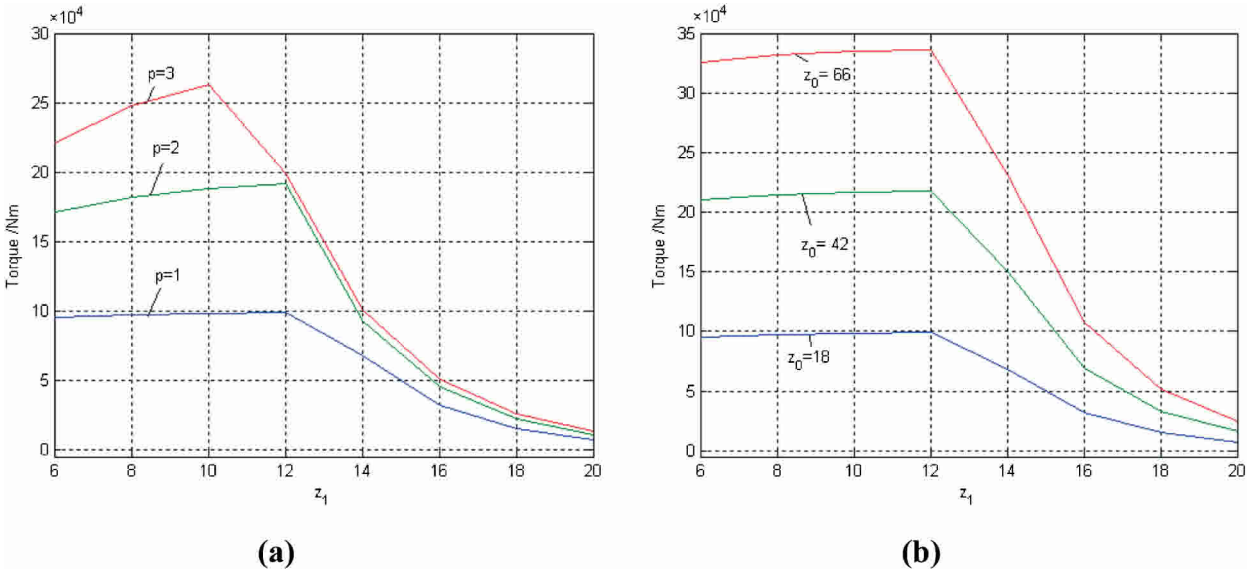

Fig. 11 Changes of the output torque along with parameters.

(4) As the stator tooth number increases, the output torque of the drive increases. This is because the gear reduction ratio of the drive increases with increasing stator tooth number. It should be noted that a change of the stator tooth number does not affect the optimum planet tooth number.
(5) In order to achieve a large output torque, a larger pole pair number and stator tooth number, and the proper planet tooth number should be selected.

7. CONCLUSIONS

Based on basic drive principles, worm coil distributions and load-carrying ability for a drive are investigated. The worm coil distributions are classified into two types: planet teeth to partial worm teeth, and worm teeth to partial planet teeth. The lead angles for the drive without an idle tooth pair are determined. Based on a coordinate transformation, the center curve of the worm groove is determined and a 3D worm model is constructed. The average output torque is presented to compare load-carrying ability for the drive with different worm coil distributions. The main results are that in order to get large output torque, a larger pole pair number and stator tooth number, and proper planet tooth number should be selected.

ACKNOWLEDGMENT

This project is supported by National Natural Science Foundation of China (No50375132).

REFERENCES

1. Kuehnle, M.R., "Toroidgetriebe," *Urkunde uber die Erteilung des deutschen Patents*, 1301682, 1966.
2. Kuehnle, M.R., Peeken, H. and Troeder, C.,"The Toroidal drive," *Mechanical Engineering*, Vol. 32, No. 2, pp. 32–39, 1981.
3. Peeken, H., Troeder, Chr. and Tooten, K.H.,"Berechnung und Messung der Lastverteilung im Toroidgeriebe," Konstruktion, Vol. l36, No. 3, pp. 81–86, 1984.
4. Tooten, K.H., "Optimierung des Kraftubertragung-sverhaltens in Getrieben mitWalzkontakten," Antriebstechnik, Vol. 24, No. 7, pp. 49–55, 1985.
5. Kuehnle, M.R., "Toroidal transmission and method and apparatus for making and assembling same," *United States Patent*, 5863273, 1999.
6. Lizhong, Xu., Then Huang and Yulin Yang, "Contact Stresses for Toroidal drive," *Journal of Mechanical Design.Transactions of the ASME*, Vol. 125, No. 3, pp. 165–168, 2003.
7. Lizhong, Xu., Jinliang, Li. and Yulin Yang, "Efficiency for Toroidal drive," in *Proceedings of the 11th World Congress in Mechanism and Machine Science*, Tianjin, China, pp. 737–740, April 1-4, 2004.
8. Lizhong, Xu. and Jin Huang, "Torque for Electromechanical Integrating Toroidal drive," *Proceedings of the I MECH E Part C Journal of Mechanical Engineering Science*, Vol. 219, No. 8, pp. 801–811, 2005.